Investigation of Halogenated Pyrimidines by X-ray Photoemission Spectroscopy and Theoretical DFT Methods

P. Bolognesi,*,† G. Mattioli,‡ P. O'Keeffe,† V. Feyer,§ O. Plekan,§ Y. Ovcharenko,†,∥ K. C. Prince,§,⊥ M. Coreno,†,⊥ A. Amore Bonapasta,‡ and L. Avaldi†,⊥

CNR-IMIP and CNR-ISM, Area della Ricerca di Roma 1, Via Salaria Km. 29.300, Monterotondo Scalo, Roma, Italy, Sincrotrone Trieste, Area Science Park, I-34012 Basovizza (Trieste), Italy, Institute of Electron Physics, 88017 Uzhgorod, Ukraine, and CNR-INFM-TASC, Gas Phase Beamline at Elettra, Area Science Park, Trieste, Italy

Received: September 3, 2009; Revised Manuscript Received: October 5, 2009

The inner shell ionization of pyrimidine and some halogenated pyrimidines has been investigated experimentally by X-ray photoemission spectroscopy (XPS) and theoretically by density functional theory (DFT) methods. The selected targets—5-Br-pyrimidine, 2-Br-pyrimidine, 2-Cl-pyrimidine, and 5-Br-2-Cl-pyrimidine—allowed the study of the effect of the functionalization of the pyrimidine ring by different halogen atoms bound to the same molecular site, or by the same halogen atom bound to different molecular sites. The theoretical investigation of the inductive and resonance effects in the C(1s) ionization confirms the soundness of the resonance model for a qualitative description of the properties of an aromatic system. Moreover, the combination of the experimental results and the theoretical analysis provides a detailed description of the effects of the halogen atom on the screening of a C(1s) hole in the aromatic pyrimidine ring.

1. Introduction

Core electrons in a molecule are essentially localized on specific atomic sites, and their binding energy is very sensitive to the chemical environment. When several atoms of the same species are present, the chemical shift of their core level binding energies provides information on molecular properties,[1] such as proton affinities,[2] chemical equilibrium, and reactivity parameters.[3] Thus, inner-shell ionization energies provide a local probe of the chemical environment of an atom in the molecule and make it possible to establish relationships between the chemical shift and chemical properties with "site dependence". This explains the widespread use of X-ray photoemission spectroscopy (XPS) since its introduction by Siegbahn.[4]

The physics and chemistry of small biological molecules are fundamental for many fields, from biotechnological applications such as sensors and heterogeneous materials[5] to astrochemistry and astrobiology. Recently, a number of XPS studies of molecules of biological interest have been reported.[6−11] This work proved that XPS can provide information on the electronic structure, partial atomic charge, and electronegativity of these molecules as well as on the molecular conformation in space. We have undertaken a gas-phase investigation of the valence and inner shell electronic structure of halogenated pyrimidines (Figure 1), probing them with laboratory sources[12,13] and synchrotron radiation. Pyrimidines are an important class of organic molecules mainly due to the fact that the pyrimidine ring forms the base structure of three nucleic acids, that is, uracil, cytosine, and thymine. Furthermore, halogenated pyrimidine bases have found applications as radiosensitizers in radiotherapy. For example, it was discovered more than 40 years ago that

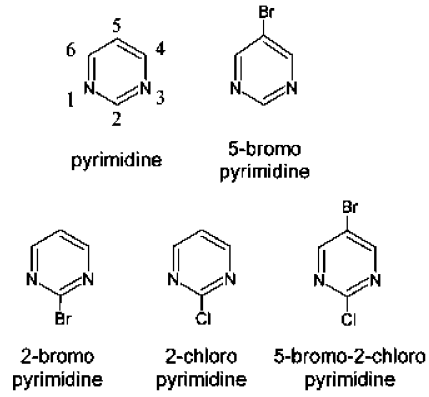

Figure 1. Schematic of the halogenated pyrimidines.

5-bromodeoxyuridine (an analogue of thymidine) enhances radiotherapeutic effects, most likely via the cascade Auger induced by the decay of the ionized halogen atom.[14,15]

In two recent works we have reported the Auger spectra[12] and the valence photoemission spectra[13] of halogenated pyrimidines. The experimental results have been compared to the theoretical predictions of the ADC model, the partial third-order quasiparticle approximation as applied to electron propagator theory[16] and a corrected density functional method based on the hybrid B3LYP functional,[17] respectively. In this study, we present the results of an XPS investigation and compare them with those achieved within the framework of a pseudopotential density functional theory (DFT) method.[18] In this method an "excited state" pseudopotential is combined with a hybrid Hartree−Fock (HF) correction to get accurate estimates of XPS binding energies.

The present work aims to provide a detailed analysis of charge density patterns corresponding to the core-hole states and clarify the effects of the halogen substitution on the electronic structure of the pyrimidine molecule.

* To whom correspondence should be addressed. E-mail: paola.bolognesi@imip.cnr.it.
† CNR-IMIP.
‡ CNR-ISM.
§ Sincrotrone Trieste.
∥ Institute of Electron Physics.
⊥ CNR-INFM-TASC.

10.1021/jp908512v CCC: $40.75
Published on Web 11/11/2009

2. Experiment

The XPS spectra were measured at the gas phase photoemission beamline of the Elettra synchrotron radiation source, Trieste,[19] using a commercial 6-channel, 150 mm hemispherical electron energy VG analyzer.[6] The light source is an undulator of period 12.5 cm, 4.5 m long. The 100% linearly polarized radiation from the undulator is deflected to the variable-angle-spherical grating monochromator[20] by a prefocusing mirror. The monochromator, placed between entrance and exit slits for photon beam resolution, consists of two optical elements: a plane mirror and a spherical grating. Five interchangeable gratings cover the energy region 13−1000 eV, with a typical resolving power of about 10000. Two refocusing mirrors after the exit slit provide a circular focus (radius about 300 μm) at the interaction region in the experimental chamber. The axis of the electron analyzer is set at the magic angle in the parallel plane, i.e. in the plane defined by the electric vector of the light and the photon propagation direction, at an angle of 54.7° with respect to the electric vector of the light. In this geometry the measurements are insensitive to the variation of the photoelectron asymmetry parameter, β.

All the samples were purchased from Sigma-Aldrich, with purity higher than 95%, and were used without further purification. At room temperature, pyrimidine is liquid, whereas all the other samples are powders. The compounds were kept in a glass vial outside the vacuum chamber and were introduced to the interaction region via a leak valve and an effusive gas line ending with a 0.8 mm hypodermic needle positioned at about 2 mm from the photon beam. At room temperature the vapor pressures of the samples were sufficient to produce a residual gas pressure in the experimental chamber varying from 9×10^{-7} to 4×10^{-6} mbar depending on the sample, enough to allow the electron spectra to be recorded without heating the sample. This procedure has the advantage of reducing contamination of the experimental apparatus and avoids the possible thermal decomposition of the biomolecules.

The C(1s) and N(1s), Cl(2p), and Br(3p) and (3d) core level spectra were measured at about 100 eV above their respective ionization thresholds, using an energy resolution of the analyzer that varies between 100 and 200 meV, depending on the measured state and its natural width. The kinetic energy of about 100 eV in the photoelectron spectra guarantees that PCI effects[21] can be neglected in the data analysis. The energy spectra were calibrated using a mixture of the molecule under study and a calibration gas with well-known XPS peaks in the same binding energy range, that is, CO_2 (C1s, $v = 0$) at 297.69 eV,[22] N_2 (N1s)[23] at 409.9 eV, Kr ($3p_{3/2}$) at 214.4 eV[24] and Kr ($3d_{5/2}$) at 93.788 eV[25] for C(1s), N(1s), Br(3p), Cl(2p), and Br(3d), respectively. We did not calibrate the transmission of the analyzer, but it is expected to be constant over the narrow energy ranges of the core level spectra. Including the bandwidth of the ionizing photon beam, the overall energy resolutions are 280 meV for the N(1s) spectra at 510 eV, 130 meV for the C(1s) spectra at 392 eV, 200 meV for the Br(3p) and Cl(2p) spectra at about 300 eV, and 160 meV for the Br(3d) spectra at 180 eV, as measured from the deconvolution of the XPS peaks of the calibration gases with known natural width.

3. Theoretical Model

It has been shown recently[26] that DFT implemented with the self-interaction correction[27] can provide reliable core ionization energies of C, N, O, and F in a number of different organic compounds. The present theoretical results have been obtained using a pseudopotential DFT method,[18] that is, an ab initio approach where core electrons are not explicitly included in a self-consistent field (SCF) calculation. A core hole is induced when the pseudopotential is generated and this "excited state" pseudopotential is then used to evaluate the relative binding energy. This approach has been used here together with a hybrid HF-DFT approach to evaluate the interelectronic interactions, namely, the B3LYP exchange-correlation functional[28] as implemented in the Quantum-ESPRESSO suite.[29]

We have investigated the properties of isolated pyrimidine molecules and their halogenated derivatives via ab initio DFT methods and a supercell approach.[29] The molecules were accommodated in large cubic supercells (25 Å^3) in order to minimize the occurrence of spurious interactions between periodically replicated cells. Total energies were calculated by using norm-conserving Troullier−Martins atomic pseudopotentials,[30] plane-wave basis sets, and the B3LYP hybrid exchange-correlation functional.[28] Satisfactorily converged results were achieved by using cutoffs of 80 Ry on the plane waves and 320 Ry on the electronic density, respectively, as well as the Γ point for the **k**-point sampling of the Brillouin zone. H (1s), C (2s) and (2p), N (2s) and (2p), Cl (3s) and (3p), and Br (4s) and (4p) electrons were treated as valence electrons. All of the inner shells were embedded in the pseudopotentials. C (1s) and N (1s) chemical shifts were theoretically estimated by total energy differences between "standard" and "core hole" calculations.[31] In the latter case, an excited state C (N) pseudopotential containing a 1s core hole was used in place of the regular pseudopotential. A different calculation was performed for each nonequivalent C (N) atom. The energy differences between the standard and core hole calculations were compared with the corresponding difference obtained for the C atom of a CO_2 molecule (N atom of a N_2 molecule), which was accommodated in every supercell and used as a reference for both the theoretical and experimental chemical shifts. The adopted hybrid setup produces very accurate predictions of XPS vertical binding energies in the systems here investigated, which improve, for example, those that can be obtained by means of the generalized gradient approximation (GGA) BLYP exchange-correlation functional and a computational setup similar to that described for the B3LYP case. This is most likely due to the fact that the amount of Hartree−Fock exact exchange inserted into the BLYP exchange-correlation functional allows one to circumvent the shortcomings in the GGA description of electron correlation, which often leads to an overestimation of the electronic delocalization. In particular, such an overestimate can affect the degree of localization of the electronic charge in the case of the excited state calculations, in which some parts of the valence electronic density has to be strongly localized in order to screen the core hole.

4. Results and Discussion

We measured experimentally the XPS spectra of the pyrimidine and halogenated pyrimidine molecules (Figure 1), namely the 5-Br-pyrimidine, 2-Br-pyrimidine, 2-Cl-pyrimidine, and 5-Br-2-Cl-pyrimidine, at the C (Figures 2 and 3, Tables 1 and 2) and N (Figure 4, Table 3) K-edges, at the Cl (Figure 6, Table 4) $L_{2,3}$- and Br $M_{2,3}$- and $M_{4,5}$-edges (Figure 7, Table 5), respectively. The energy range of the Gas phase beamline did not allow access to Br and Cl levels deeper than Br(3p) and Cl(2p).

The C(1s) and N(1s) XPS spectra of pyrimidine and halogenated pyrimidines are reported in Figures 2 and 4, respectively, where they are compared with the results of the DFT calculations. The N(1s) spectra have only one peak, due

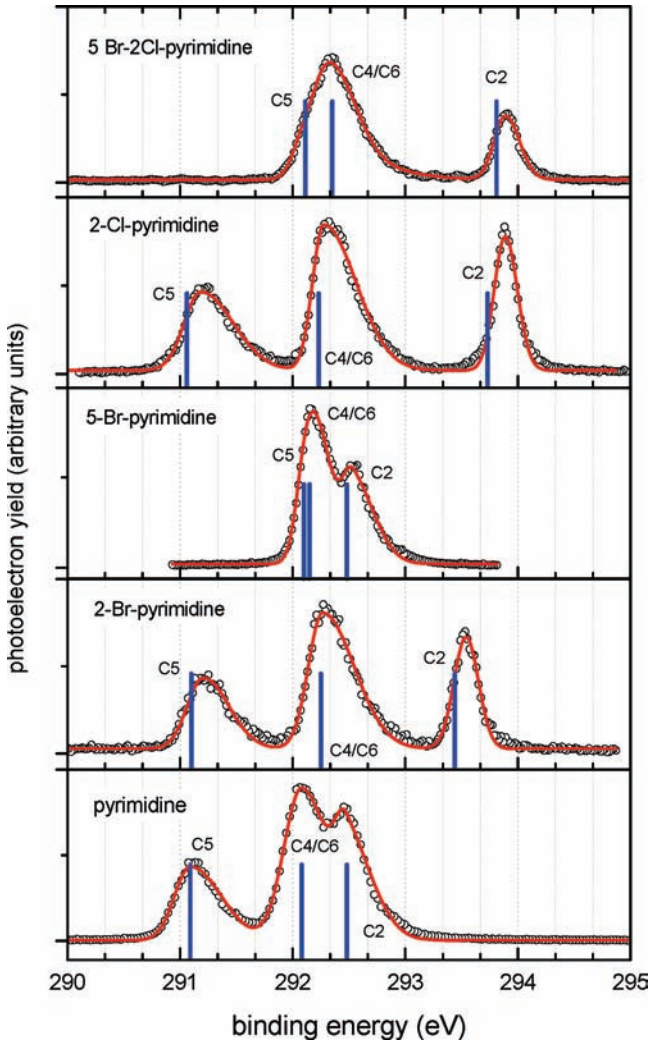

Figure 2. C(1s) XPS spectra of pyrimidine and halogenated pyrimidines: experimental results (open dots), fit with asymmetric Gaussian lineshapes (full line) and DTF theoretical calculations.

to the two equivalent N atoms in the pyrimidine ring. Each C(1s) spectrum is composed of three main features, corresponding to the ionization of the C atom in the three nonequivalent sites of the molecules—C2, C4/C6, and C5 (see Figure 1). Each of these XPS peaks is most likely the convolution of an undefined number of overlapping and unresolved vibrational progressions, which are well-known to contribute significantly to the line broadening in core photoelectron spectra.[32] The resulting asymmetric profile of each peak has been approximated in the fitting procedure by an asymmetric Gaussian function with all parameters (i.e., the position of the centroid, the area and the low/high energy side widths) used as free parameters. This procedure provides a reasonable description of the spectra with only small discrepancies on the tail of the peaks. The centroid of each peak has been assumed to be the binding energy of the state and is reported in Table 1 together with the areas of the peaks extracted from the fit. In the case of the C4/C6 and C5 peaks of the 5-Br- and 5-Br-2-Cl-pyrimidine, the overlap of the features hampers an accurate fit. Thus, the order of the C4/C6 and C5 peaks as well as their relative intensities in both molecules may have a larger uncertainty (Table 1). A previous determination of the binding energies of the nonequivalent C atoms in pyrimidine was reported in ref 33. Very good agreement between the two sets of data exists. Values of the C(1s) binding energy of pyrimidine, 5-Br-pyrimidine, and 2-Cl-pyrimidine molecules were also estimated from the Auger spectra and ADC calculations of the double ionization potentials.[34] The differences between those values and the present ones, that in some cases amount to 1 eV, are mainly due to the large uncertainty associated with the measurement of the broad bands of the Auger spectra. Within 10%, the experimental relative intensities follow the expected trend, being proportional to the number of equivalent atoms in the molecule, that is, intensity(C2)/intensity(C4/C6)/intensity(C5) $\approx$ 0.5:1:0.5 (see Table 1). Theoretical results are reported together with the experimental ones in Tables 1−3. An overview of the experimental and theoretical binding energies for the nonequivalent C atoms in all investigated molecules are reported in the correlation diagrams of Figure 3.

Remarkably good agreement between the theoretical predictions and experimental data is observed, the differences are on average about 0.1 eV and never exceed 0.15 eV. In the case of 5-Br-pyrimidine the calculation predicts a different order for the C5 and C4/C6 peaks, however the uncertainty in the assignment of these two peaks due to their overlap may explain this difference. The general effect of the halogenation is to produce a shift of all the C(1s) binding energies toward higher values. The shift is significantly more pronounced for the carbon site directly involved in the halogenation, due to the electrophilic behavior of the Cl and Br atoms with respect to the C atoms of the pyrimidine aromatic ring. In this regard, slightly larger effects have been observed in the case of Cl-substituted C atoms, because of the higher electronegativity of Cl than Br. A similar, but weaker effect, can be observed in the N(1s) experimental spectra (Figure 4 and Table 3). Within the experimental uncertainty, it appears that the positive shift of the N(1s) peak can be doubled in the case of the doubly halogenated 5-Br-2-Cl-pyrimidine. The increased binding energies of the C and N (1s) levels are correlated with decreased binding energy of the halogen core levels, compared to the same quantity measured in the case of the Cl_2 and Br_2, which are homonuclear molecules (see Tables 4 and 5). This is related to a charge transfer from the pyrimidine aromatic ring to the Cl or Br atoms.

A more refined analysis of the present experimental and theoretical results can be attempted by using two elementary models related to a stronger, isotropic inductive effect, which involves the atoms nearer to a substituent more than the farther ones and a weaker, anisotropic resonance effect running along the π-conjugated bonds, respectively.[35] These models, widely used to illustrate the properties of aromatic compounds, are applied here in the analysis of the screening of a core hole. Let us consider first the experimental results of Figure 3 and Table 2. The evolution of the binding energies for the C atoms in the different molecules can be mainly accounted for by the inductive effect. However, there is an interesting exception in the case of the C4/C6 binding energy. This energy increases in the 2-Cl- and 2-Br-pyrimidines with respect to pyrimidine, then it decreases in the 5-Br-pyrimidine and increases again in the 5-Br-2-Cl-pyrimidine. Two related observations can be made: (i) the decrease of the C4/C6 chemical shift from the 2-Br- to the 5-Br-pyrimidine (see Table 2) is unexpected according to the inductive effect that would indeed suggest an opposite behavior (the 5-Br is closer to the C4 and C6 atoms than the 2-Br); and (ii) in the 5-Br-2-Cl-pyrimidine the sum of the inductive effects of the Cl and Br substituents would lead to a larger C4/C6 chemical shift relative to pyrimidine than the measured value of +0.25 eV. This observation can be explained by the resonance effect. In a formal schematization such an effect implies that the halogen can carry a positive charge, gives

TABLE 1: Theoretical (Binding Energies, BE) and Experimental (BE and Relative Intensities) Results for the C(1s) of Pyrimidine and Halogenated Pyrimidines, Compared with Previous Results[a]

	present results			previous results		
C 1s state	BE (eV) experiment	rel. int. experiment	BE (eV) theory	BE (eV)[33] theory	BE (eV)[33] experiment	BE (eV)[37] theory
CO_2 (C1s, $v = 0$)	297.69 ± 0.02					
pyrimidine	291.09 ± 0.04	0.52 ± 0.04	291.09 (C5)	290.93	291.1	290.35
	292.08 ± 0.02	1.00 ± 0.05	292.08 (C4/C6)	291.79	292.0	291.14
	292.48 ± 0.03	0.53 ± 0.07	292.48 (C2)	292.14	292.4	291.45
2-chloro pyrimidine	291.18 ± 0.03	0.60 ± 0.02	291.06 (C5)			
	292.27 ± 0.04	1.00 ± 0.04	292.23 (C4/C6)			
	293.88 ± 0.03	0.49 ± 0.03	293.73 (C2)			
2-bromo pyrimidine	291.20 ± 0.04	0.47 ± 0.02	291.10 (C5)			
	292.26 ± 0.02	1.00 ± 0.02	292.25 (C4/C6)			
	293.54 ± 0.02	0.44 ± 0.03	293.44 (C2)			
5-bromo pyrimidine	292.19 ± 0.06	0.45 ± 0.04	292.10 (C5)			
	292.13 ± 0.08	1.00 ± 0.06	292.15 (C4/C6)			
	292.53 ± 0.06	0.66 ± 0.10	292.48 (C2)			
5-bromo-2chloro pyrimidine	292.11 ± 0.07	0.32 ± 0.05	292.11 (C5)			
	292.33 ± 0.07	1.00 ± 0.04	292.35 (C4/C6)			
	293.89 ± 0.02	0.36 ± 0.01	293.81 (C2)			

[a] The uncertainty in the present theoretical calculations is estimated to be 0.1 eV.

TABLE 2: C(1s) Experimental and Theoretical Chemical Shifts of the C2, C4/C6, C5 Sites of Halogenated Pyrimidines Reported with Respect to the Same Atoms in the Pyrimidine Molecule

	chemical shift (eV)							
		2-Cl pyrimidine		2-Br pyrimidine		5-Br pyrimidine		5-Br-2Cl pyrimidine	
	pyrimidine	expt.	th.	expt.	th.	expt.	th.	expt.	th.
C2	0	+1.40	+1.25	+1.06	+0.96	+0.05	0	+1.41	+1.33
C4/C6	0	+0.19	+0.15	+0.18	+0.17	+0.11	+0.07	+0.25	+0.25
C5	0	+0.09	−0.03	+0.11	+0.01	+1.04	+1.01	+1.02	+1.02

electronic charge to the aromatic system, and forms a double bond with its C neighbor. The additional electron can be considered to be preferably localized in ortho and para positions with respect to the halogen. In the case of the 5-Br-pyrimidine, the resonance effect reduces the inductive effect of Br on the C4 and C6 atoms occupying ortho positions with respect to the halogenated C5. The resonance effect produces indeed better screening of the core hole, thus accounting for the decrease of the chemical shift. Similar results have been reported by Clark et al. in the case of chloro- and dichloro-benzenes.[36] A complementary consideration can be made in the case of the N(1s) binding energies: the N atoms are in meta positions with respect to the Br-substituted C5 atom in the 5-Br-2-Cl-pyrimidine. No resonance contributions of the Br can improve the screening of the core hole, so its inductive contribution roughly doubles the N shift in the doubly halogenated molecule. It can be noted that the resonance effects can also account for small differences observed in the spectrum of the 5-Br-pyrimidine. The balancing of the inductive effect by the resonance one indeed leads to a similar increase of the C4/C6 binding energies. This, together with the small increase of the C2 binding energy and the large one of the C5 binding energy,

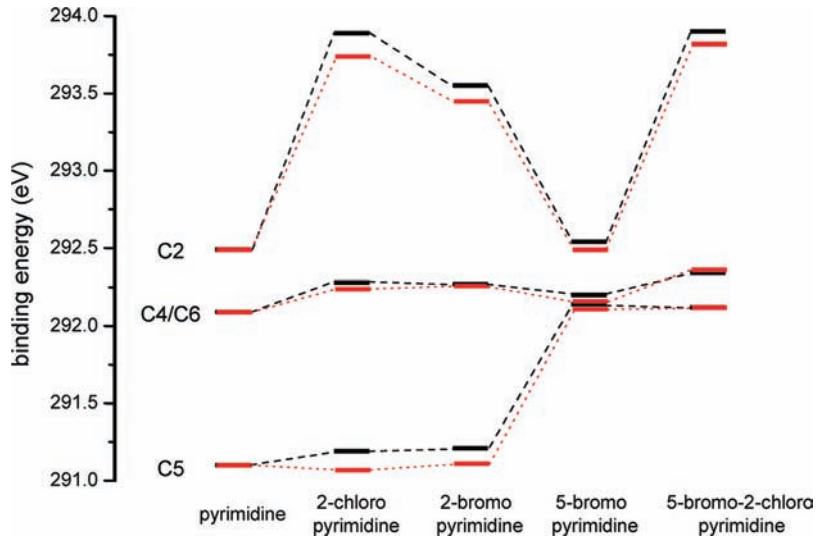

Figure 3. Correlation diagram for the C(1s) pyrimidine and halogenated pyrimidines from the experimental measurements (in black) and DFT calculations (in red).

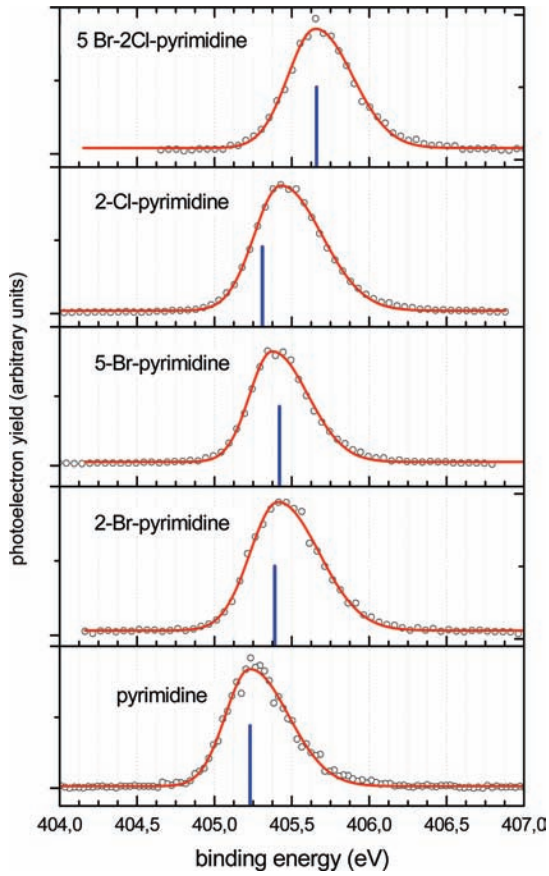

Figure 4. N(1s) XPS spectra of pyrimidine and halogenated pyrimidines compared to the DFT calculations.

TABLE 3: N(1s) Experimental and Theoretical Binding Energies of Pyrimidine and Halogenated Pyrimidines and the Corresponding Chemical Shifts Reported with Respect to the Pyrimidine Molecule

N 1s state	BE (eV) experiment.	BE (eV) theory	chemical shift (eV) experiment	chemical shift (eV) theory
N_2 (N1s)	409.9 ± 0.04			
pyrimidine	405.23 ± 0.04	405.14	0	0
2-chloro pyrimidine	405.43 ± 0.04	405.20	0.20	0.06
2-bromo pyrimidine	405.41 ± 0.04	405.30	0.18	0.16
5-bromo pyrimidine	405.37 ± 0.04	405.33	0.14	0.19
5-bromo-2chloro pyrimidine	405.65 ± 0.04	405.57	0.42	0.43

TABLE 4: Cl(2p) Binding Energies of Halogenated Pyrimidines

Cl	$2p_{3/2}$	$2p_{1/2}$
2-chloro pyrimidine	206.24 ± 0.01	207.87 ± 0.01
5-bromo-2chloro pyrimidine	206.24 ± 0.01	207.85 ± 0.01
Cl_2[39]	207.85	209.4

results in the three binding energies being about 300 meV, thus hampering a complete deconvolution of the experimental XPS spectrum.

Now, let us consider how the inductive and resonance models apply when discussing the theoretical results and their comparison with the experiment. As already stated above, generally good agreement has been found between the theoretical and the experimental C (1s) results (Tables 1 and 2, and Figure 3) with discrepancies smaller than 0.15 eV. The present theoretical data for the pyrimidine molecule are in better agreement with experiments than previous results obtained using a hybrid DFT method[37] and the ΔKohn−Sham calculations.[32] As expected the first of these calculations is less accurate due to the application of the "meta Koopmans' Theorem" which shows an error of up to 1.0 eV in the IP of the C2 (1s) level, but produces core binding energies for all atoms in the molecule with a single calculation. The ΔKohn−Sham method in ref 32, on the other hand, is a Δ method like the one used in this work (as a result, it requires $n + 1$ calculations, where n is the number of core-hole states) and indeed has a maximum deviation from the experiments of 0.34 eV. In both methods, the largest shift of the halogenated carbon and the trend of the C4/C6 experimental shifts are reproduced by theory.

To perform a deeper analysis of the theoretical results based on the resonance and inductive effects, we have considered the displacement of the electron charge density in molecules with a C(1s) core hole. This has been investigated by analyzing difference electron density maps obtained by subtracting the *valence* electronic density of a ground state calculation from the *valence* electronic density of the corresponding core hole state calculation. The difference map (Figure 5) shows blue-colored positive zones, where some charge density is accumulated in order to screen the core hole, and red-colored negative zones, where that electron density has been reduced. Three series of difference density maps are shown in Figure 5. The first group (Figures 5A−C) focuses on different locations of the C(1s) hole in the 2-bromo-pyrimidine molecule. As expected, all the C(1s) core holes are screened by an almost spherical charge distribution: the three biggest blue spots in Figures 5A−C are related to the core holes in the C5, C4, and C2 positions, respectively. This screening charge is drained from the rest of the molecule in two modes. Part of the red zones is symmetrically oriented toward the core hole position, and the nearest neighbors are much more affected than those farther away. This is the screening due to the inductive effect, which, moreover, mixes σ and π components. On the other hand, different red zones (partially overlapping the former ones) show an evident π character. This corresponds to the resonance contribution to the screening (similar to the one discussed above and related to the halogen substitution) coming from the para position with respect to the core hole. This is always appreciable, for both the C (Figures 5A and C) and N atoms (Figure 5B), whereas no contribution is given from atoms in meta positions. As for the Br atom, we can observe three different patterns. When the core hole is created in the C2 position (Figure 5C), an inductive effect dominates the electron displacement of the charge density (the red spot has clear *sp* character). On the other hand, in the case of the C5 position (Figure 5A), a resonance contribution to the screening of the core hole clearly involves a π-conjugated orbital. This clarifies the two-fold role of halogens when substituting H atoms in aromatic compounds. Despite their clear and mainly charge-draining role, they extend the π-conjugation forming a halogen−carbon double bond, and enlarge the aromatic system. Finally, in the case of the C4/C6 position (Figure 5B), the Br atom is not involved in the screening of the core hole due to its distance from the hole, which weakens the inductive contribution, and due to the meta position, which inhibits the resonance contribution. The above analysis clarifies the roles of inductive and resonance effects in the 2-Br-pyrimidine. Experiment and theory (Table 2) indicate the same trend of the chemical shift in the C2, C4/C6, and C5 series. A second group of maps (Figures 5C−F) concerns the C2 position in different molecules, namely pyrimidine, and its 2-Br-, 2-Cl-, and 5-Br-2-Cl- derivatives. In this case, we can compare the effects of single and double halogen substitutions of H atoms.

TABLE 5: Br(3p and 3d) Binding Energies of Halogenated Pyrimidines

Br	$3p_{3/2}$	$3p_{1/2}$	$3d_{5/2}$	$3d_{3/2}$
5-bromo pyrimidine	190.13 ± 0.01	196.81 ± 0.01	76.791 ± 0.010	77.829 ± 0.010
2-bromo pyrimidine	189.51 ± 0.01	196.20 ± 0.02	76.217 ± 0.010	77.253 ± 0.010
5-bromo-2chloro pyrimidine	190.40 ± 0.01	197.035 ± 0.03	76.930 ± 0.010	77.961 ± 0.010
Br_2			77.40[40]	

The pyrimidine aromatic ring, with the two electrophilic N substituents, is not expected to show drastic displacements of the aromatic charge density because of the presence of the halogen atoms. In fact, we have already pointed out that an appreciable shift in the XPS binding energies is measured and calculated only in the case of the C atoms directly bound to the Cl or Br atoms. Nonetheless, the above-mentioned density maps demonstrate how the presence of the halogen atoms affects the

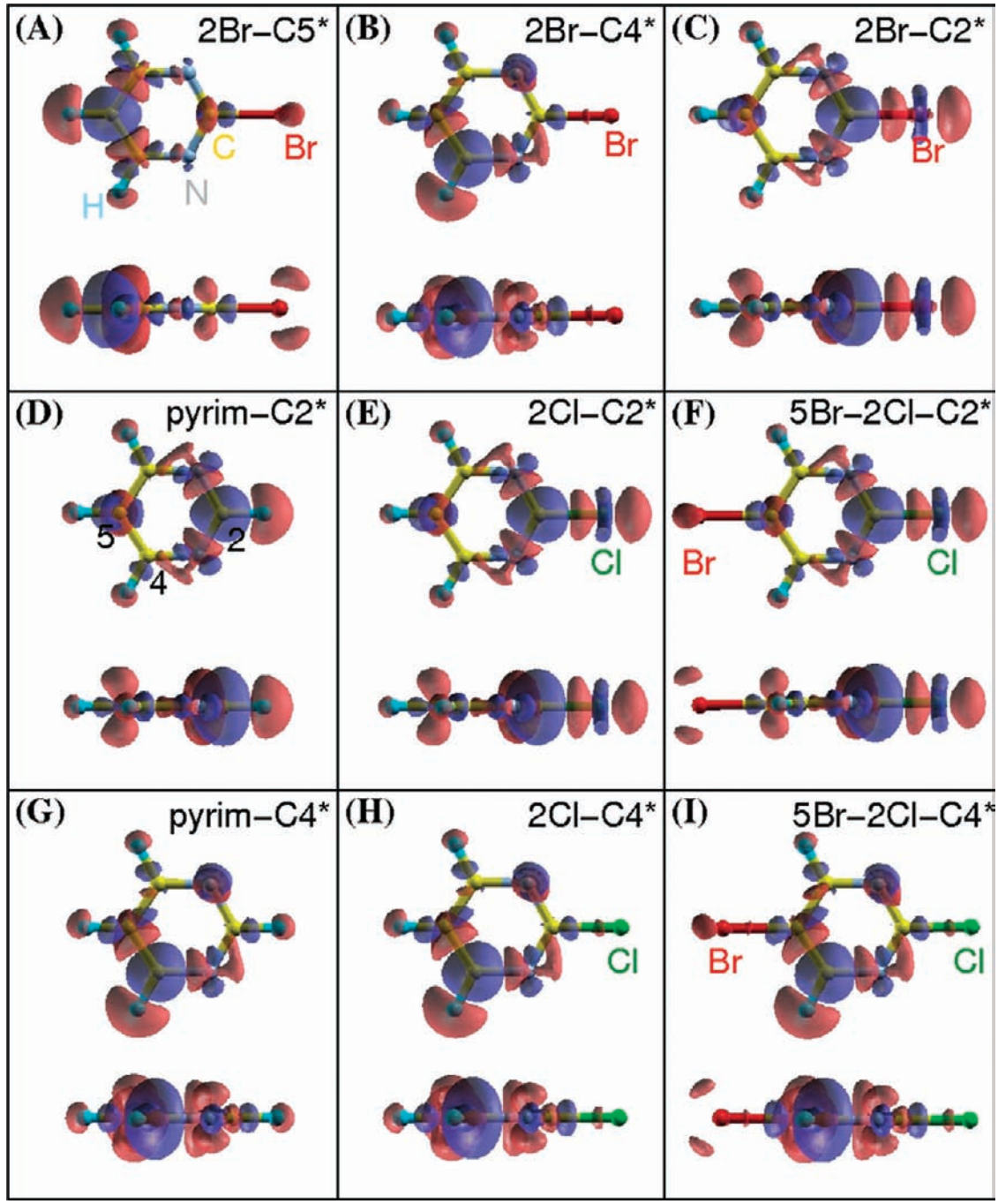

Figure 5. Difference density maps (top and side view) of "standard" versus "core hole" calculations (see the text): (A) C5 position of the 2-bromo-pyrimidine; (B) C4 position of the 2-bromo-pyrimidine; (C) C2 position of the 2-bromo-pyrimidine; (D) C2 position of the pyrimidine; (E) C2 position of the 2-chloro-pyrimidine; (F) C2 position of the 5-bromo-2-chloro-pyrimidine. (G) C4 position of the pyrimidine; (H) C4 position of the 2-chloro-pyrimidine; (I) C4 position of the 5-bromo-2-chloro-pyrimidine. Blue and red zones represent positive and negative isosurfaces, respectively, of electronic density sampled at 0.005 electrons/au^3.

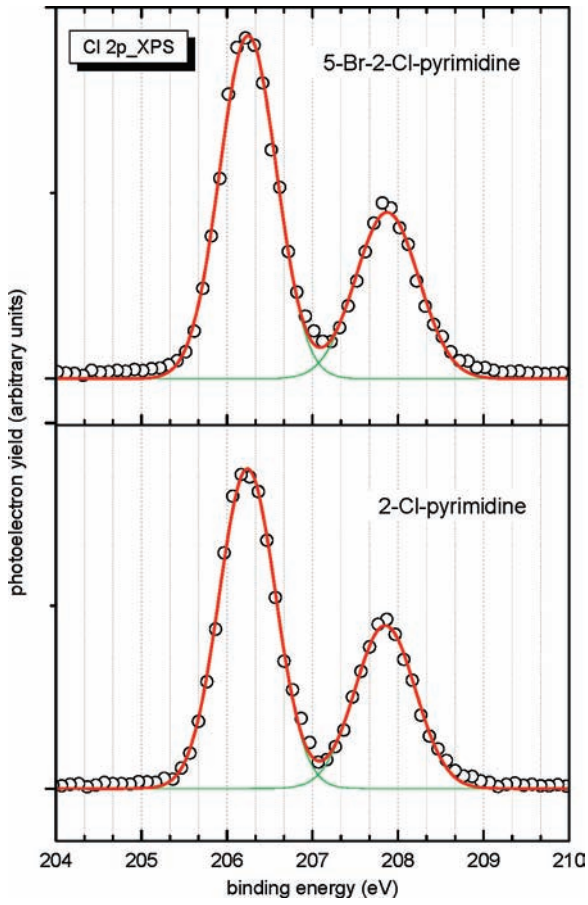

Figure 6. Cl(2p) XPS spectra of 2-chloro and 5-bromo-2chloro-pyrimidines.

aromatic ring by draining a certain amount of charge density. In particular, we note that in pyrimidine (Figure 5D) a contribution to the screening of the C2 hole comes from the farthest C5 atom and not from C4 and C6 ones. That contribution is explained by a resonance effect involving the C5 atom in the para position with respect to the C2 hole. Looking at this C5 resonance contribution, we observe that it persists in the 2-Cl compound (Figure 5E), while it decreases, as shown by a shrinkage of the red spot, due to the inductive effect in the case of the 5-Br-2-Cl- one (Figure 5F). Finally, Figures 5G−I show the results relative to the C4/C6 positions in pyrimidine, and 2-Cl- and 5-Br-2-Cl-pyrimidine. These results show that a 2-Cl in the meta position with respect to the C4 core hole does not contribute to the hole screening (Figure 5H), whereas a 5-Br in the ortho position with respect to the C4 core hole does contribute (Figure 5I). This confirms the occurrence of a resonance effect balancing the inductive one, proposed in the above discussion to explain the peculiar chemical shifts observed for these molecules. In this case, the characteristic trend found for the C4/C6 chemical shifts in the cases of the 2Cl- and 5-Br-2-Cl-pyrimidines as well as of the 2-Br- and 5-Br-pyrimidines are fully reproduced by the theoretical results (see Table 2).

For the sake of completeness, the XPS experimental spectra of the Cl and Br core levels together with the results of their fits are reported in Figures 6 and 7 and Tables 4 and 5, respectively. In these cases symmetric Gaussian and Lorentzian lineshapes were adopted. The Lorentzian line shape of the Br(3p) results from the natural width of the 3p state, which is larger than the instrumental resolution. For the other halogen core levels, a Gaussian line shape is more suited, due to the comparable size of these two quantities. The literature binding energies of the same states in Cl_2 and Br_2 have been reported

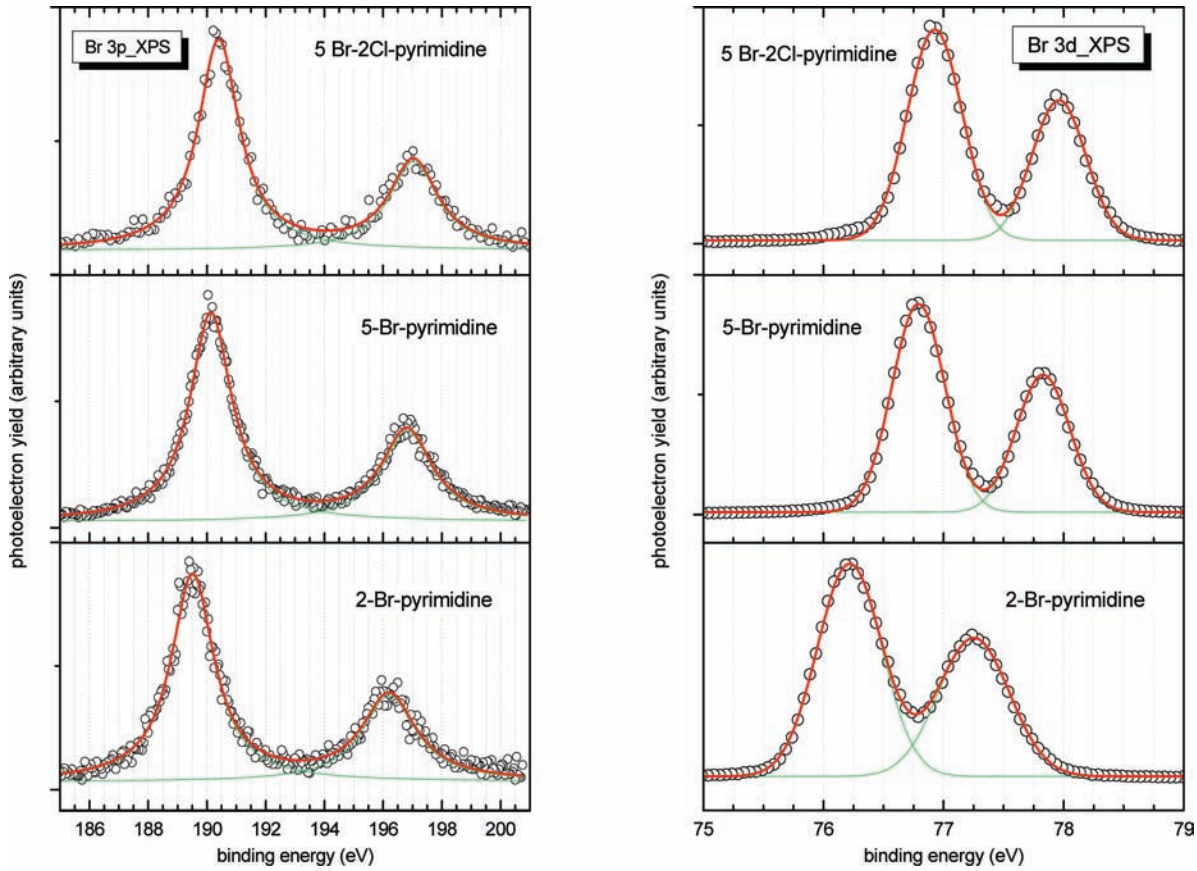

Figure 7. (a) Br(3p) and (b) Br(3d) XPS spectra of 5-bromo and 5-bromo-2chloro-pyrimidines.

for reference in Tables 4 and 5. As already mentioned, the effect of the stronger electronegativity of the halogen atoms, compared to the substituted hydrogen, produces in all the investigated cases a negative shift, that is, a decrease, in the binding energies of the Cl and Br atoms of halogenated pyrimidines with respect to the corresponding Cl_2 and Br_2 homonuclear molecules. The measured spin−orbit splittings for the Cl($2p_{3/2,1/2}$), Br($3p_{3/2,1/2}$), and Br($3d_{5/2,3/2}$) states are 1.62 ± 0.01, 6.67 ± 0.02, and 1.04 ± 0.05 eV, respectively. They do not depend on the particular molecule within the present experimental resolution and accuracy.

The estimated natural widths of both spin−orbit split states, after taking account of the instrumental resolution, are: (0.79 ± 0.05) eV for Cl(2p), and (1.7 ± 0.15) eV and (0.50 ± 0.05) eV for Br(3d). For Br 3p, the widths are (1.7 ± 0.15) eV and (2.1 ± 0.15) eV for Br ($3p_{3/2}$ and $3p_{1/2}$ components respectively. The larger width of the Br $3p_{1/2}$ component compared with $3p_{3/2}$ is similar to the Kr 3p case where the $3p_{1/2}$ photoelectron line was observed to be broader (1.80 eV) than the $3p_{3/2}$ line (1.48 eV).[38] It is due to an additional super Auger Coster−Kronig transition that is energetically forbidden for the $3p_{3/2}$ hole state.

5. Conclusions

The XPS spectra of pyrimidine and some halogenated pyrimidines—namely, 5-Br-pyrimidine, 2-Br-pyrimidine, 2-Cl-pyrimidine, and 5-Br-2-Cl-pyrimidine—have been measured and investigated theoretically by DFT calculations. A remarkably good agreement between theoretical and experimental chemical shifts has been observed. The results show that, due to the higher electronegativity of the halogen atoms compared to substituted hydrogen, all the carbon and nitrogen atoms in the six-member ring are affected by halogenation and their binding energies shift toward higher energies. As expected, the largest shifts are those of the halogenated carbon sites, with typical values of the order of 1.0−1.4 eV with respect to the same site in the pyrimidine molecule. The theoretical picture emerging from the study of the inductive and resonance effects on the C(1s) hole screening confirms the soundness of the description of the properties of an aromatic system given by the resonance model. Present results show indeed that the rearrangements of the electronic charge occurring in the pyrimidine derivatives to screen a core hole estimated by ab initio methods are in very good agreement with the qualitative picture given by the inductive-resonance model. In some cases, the observed shift is explained only by the interplay of the two effects.

The present theoretical and experimental results give a detailed description of the effects of halogen substitutions in the pyrimidine molecule as for the screening of the C(1s) hole located at different positions of the aromatic ring. Because pyrimidine and halogenated pyrimidines are the building block of DNA/RNA bases and of several pharmaceutical compounds, these new results contribute to the databank needed to understand the physical and chemical origin of the photoinduced processes and damages in these large biological molecules.

Acknowledgment. G.M. and A.A.B. are glad to thank Professor P. Giannozzi for helpful discussions about the theoretical XPS technique and the CINECA consortium for computational support. The authors thank the Elettra support program for Italian users, and the staff of Elettra for providing high quality light. This research was partly supported by a Marie Curie Reintegration Grant with the 7th European Community Framework Programme.

References and Notes

(1) Svensson, S. *J. Phys. B* **2005**, *38*, S821.
(2) Mills, B. E.; Martin, R. L.; Shirley, D. A. *J. Am. Chem. Soc.* **1976**, *98*, 2380.
(3) Lindberg, B.; Svensson, S.; Malmquist, P. A.; Basilier, E.; Gelius, U.; Siegbahn, K. *Chem. Phys. Lett.* **1976**, *40*, 175.
(4) Siegbahn, K. *ESCA Applied to Free Molecules*; North-Holland Publishing: Amsterdam: London, 1969.
(5) Cavalleri, O.; Gonella, G.; Terreni, S.; Vignolo, M.; Floreano, L.; Morgante, A.; Canepa, M.; Rolandi, R. *Phys. Chem. Chem. Phys.* **2004**, *6*, 4042.
(6) Plekan, O.; Feyer, V.; Richter, R.; Coreno, M.; de Simone, M.; Prince, K. C.; Carravetta, V. *Chem. Phys. Lett.* **2007**, *442*, 429.
(7) Plekan, O.; Feyer, V.; Richter, R.; Coreno, M.; de Simone, M.; Prince, K. C.; Cararvetta, V. *J.Phys. Chem. A* **2007**, *111*, 10988.
(8) Feyer, V.; Plekan, O.; Richter, R.; Coreno, M.; Prince, K. C.; Carravetta, V. *J. Phys. Chem. A* **2008**, *112*, 7806.
(9) Plekan, O.; Feyer, V.; Richter, R.; Coreno, M.; de Simone, M.; Prince, K. C.; Trofimov, A. B.; Gromov, E. V.; Zaytseva, I. L.; Schirmer, J. *Chem. Phys.* **2008**, *347*, 360.
(10) Brown, R. S.; Tse, A.; Vedera, J. C. *J. Am. Chem. Soc.* **1980**, *102*, 1174.
(11) Powis, I.; Rennie, E. E.; Hergenhahn, U.; Kugeler, O.; Bussy-Socrate, R. *J.Phys. Chem. A* **2003**, *107*, 25.
(12) Storchi, L.; Tarantelli, F.; Veronesi, S.; Bolognesi, P.; Fainelli, E.; Avaldi, L. *J. Chem. Phys.* **2008**, *129*, 154309.
(13) O'Keeffe, P.; Bolognesi, P.; Catone, D.; Zema, N.; Turchini, S.; Casavola, A.; Avaldi, L. *Mol. Phys.* **2009**, *107*, 2025.
(14) Dewey, W. C.; Humphrey, R. M. *Radiat. Res.* **1965**, *26*, 538.
(15) Sano, K.; Hoshino, T.; Nagai, M. *J. Neurosurg.* **1968**, *28*, 530.
(16) Ortiz, V. *J. Chem. Phys.* **1996**, *104*, 7599.
(17) Gritsenko, O. V.; Braida, B.; Baerends, E. J. *J. Chem. Phys.* **2003**, *119*, 1937.
(18) Payne, M. C.; Teter, M. P.; Allan, D. C.; Arias, T. A.; Joannopulos, J. D. *Rev. Mod. Phys.* **1992**, *64*, 1045.
(19) Prince, K. C.; Blyth, R. R.; Delaunay, R.; Zitnik, M.; Krempasky, J.; Slezak, J.; Camilloni, R.; Avaldi, L.; Coreno, M.; Stefani, G.; Furlani, C.; de Simone, M.; Stranges, S. *J. Synchotron Rad.* **1998**, *5*, 565.
(20) Melpignano, P.; Di Fonzo, S.; Bianco, A.; Jark, W. *Rev. Sci. Instrum.* **1995**, *66*, 2125.
(21) van der Straten, P.; Mongerstern, R.; Niehaus, A. *Z. Phys.* **1988**, *D8*, 35.
(22) Hatamoto, T.; Matsumoto, M.; Liu, X.-J.; Ueda, K.; Hoshino, M.; Nakagawa, K.; Tanaka, T.; Tanaka, H.; Ehara, M.; Tamaki, R.; Nakatsuji, H. *J. Electron Spectrosc. Relat. Phenom.* **2007**, *155*, 54.
(23) Kempgens, B.; Kivimäki, A.; Neeb, M.; Köppe, H. M.; Bradshaw, A. M.; Feldhaus, J. *J. Phys. B: At. Mol. Phys.* **1996**, *29*, 5389. Darrah Thomas, T.; Robert, W.; Shaw, Jr. *J. Electron Spectrosc. Relat. Phenom.* **1974**, *5*, 1081.
(24) Steinberger, I. T.; Teodorescu, C. M.; Gravel, D.; Flesch, R.; Wassermann, B.; Reichardt, G.; Hutchings, C. W.; Hitchcock, A. P.; Ruhl, E. *Phys. Rev B* **1999**, *60*, 3995.
(25) Tronc, M.; King, G. C.; Read, F. H. *J. Phys. B: At. Mol. Phys* **1977**, *12*, 137.
(26) Tu, G.; Carravetta, V.; Vahtras, O.; Ågren, H. *J. Chem. Phys.* **2007**, *127*, 174110.
(27) Perdew, J. P.; Zunger, A. *Phys. Rev. B* **1981**, *23*, 5048.
(28) Becke, A. D. *J. Chem. Phys.* **1993**, *98*, 5648. Lee, C.; Yang, W.; Parr, R. G. *Phys. Rev. B* **1988**, *37*, 785.
(29) Giannozzi, P.; et al. *J. Phys.: Condens. Matter* **2009**, *21*, 395502. http://www.quantum-espresso.org.
(30) Troullier, N.; Martins, J. L. *Phys. Rev. B* **1991**, *43*, 1993.
(31) Pehlke, E.; Scheffler, M. *Phys. Rev. Lett.* **1993**, *71*, 2338. Bianchettin, L.; Baraldi, A.; de Gironcoli, S.; Lizzit, S.; Petaccia, L. *Phys. Rev. B* **2006**, *74*, 045430.
(32) Neeb, M.; Kempgens, B.; Kivimäki, A.; Köppe, H. M.; Maier, K.; Hergenhahan, U.; Piancastelli, M. N.; Rüdel, A.; Bradshaw, A. M. *J. Electron Spectrosc. Relat. Phenom.* **1998**, *88−91*, 19.
(33) Vall-llosera, G.; Gao, B.; Kivimäki, A.; Coreno, M.; Álvarez Ruiz, J.; de Simone, M.; Ågren, H.; Rachlew, E. *J. Chem. Phys.* **2008**, *128*, 044316.
(34) Storchi, L.; Tarantelli, F.; Veronesi, S.; Bolognesi, P.; Fainelli, E.; Avaldi, L. *J. Chem. Phys.* **2008**, *129*, 154309.
(35) Carey, F. A.; Sundberg, R. J. *Advanced Organic Chemistry*; Plenum Publishing Corporation: 1990.
(36) Clark, D. T.; Kilcast, D.; Adams, D. B.; Musgrave, W. K. R. *J. Electron Spectrosc. Relat. Phenom.* **1975**, *6*, 117.
(37) Wang, F.; Zhu, Q.; Ivanova, E. *J. Synchrotron Rad.* **2008**, *15*, 624.
(38) Svensson, S.; Mårtensson, N.; Basilier, E.; Malmquist, P. A.; Gelius, U.; Siegbahn, K. *Phys. Scr.* **1976**, *14*, 141.
(39) Travnikova, O.; Fink, R. F.; Kivimäki, A.; Zhuo Bao, D. C.; Piancastelli, M. N. *Chem. Phys. Lett.* **2006**, *426*, 452.
(40) Bakke, A. A.; Chen, H.-W.; Jolly, W. L. *J. Electron Spectrosc. Relat. Phenom.* **1980**, *20*, 333.

JP908512V